ORIGINAL ARTICLE

Second Harmonic Generation Microscopy: A Tool for Spatially and Temporally Resolved Studies of Heat Induced Structural Changes in Meat

Dagmar A. Brüggemann · Jonathan Brewer · Jens Risbo · Luis Bagatolli

Abstract Myofibers and collagen show non-linear optical properties enabling imaging using second harmonic generation (SHG) microscopy. The technique is evaluated for use as a tool for real-time studies of thermally induced changes in thin samples of unfixed and unstained pork. The forward and the backward scattered SHG light reveal complementary features of the structures of myofibers and collagen fibers. Upon heating the myofibers show no structural changes before reaching a temperature of 53 °C. At this temperature the SHG signal becomes extinct. The extinction of the SHG at 53 °C coincides with a low-temperature endotherm peak observable in the differential scanning calorimetry (DSC) thermograms. DSC analysis of epimysium, the connective tissue layer that enfold skeletal muscles, produces one large endotherm starting at 57 °C and peaking at 59.5 °C. SHG microscopy of collagen fibers reveals a variability of thermal stability. Some fibers show severe shrinkage at 57 °C, before the signal for most of them vanishes between 59 °C and 61 °C and thus coinciding with the endotherm of the thermograms. However, in some areas, strong SHG signals from collagen can be visualized even after prolonged heating to 67 °C and thus indicating regions of much higher thermal stability. It is seen that the benefits of the structural and temporal information available from SHG microscopy reveals complementary information to a traditional DSC measurement and enables a more complete understanding of the thermal denaturation process.

D. A. Brüggemann (✉) · J. Risbo
Department of Food Science, Faculty of Life Sciences,
University of Copenhagen,
Rolighedsvej 30,
1958 Frederiksberg C, Denmark
e-mail: dab@life.ku.dk

J. Brewer · L. Bagatolli
Membrane Biophysics and Biophotonics Group,
Department of Biochemistry and Molecular Biology,
University of Southern Denmark,
Campusvej 55,
5230 Odense M, Denmark

Introduction

Detailed knowledge about the mechanism of the interaction of molecules in relation to microstructures is of prime importance in order to produce meat and meat products of requested structure, safety, and overall quality. Therefore, classical microscopy has traditionally been an important tool in the field of food science. In recent years, fluorescence microscopy in combination with confocal scanning laser microscopy has become the method of choice for visualization of less abundant molecules[1]. The use of light, rather than traditional histological sectioning methods provides a minimally invasive method of visualizing food structures and can be used to study static phenomena as well as dynamic processes. Nevertheless, most of the fluorescence-based bioimaging schemes require that the specimen contains either intrinsic or extrinsic fluorescent probes in order to produce contrast. Recently, the development of microscopy techniques based on non-linear optical phenomena, such as second harmonic generation (SHG), has enabled imaging of structures where the significant contrast is based on combinations of the local chemistry, the organization, and/or the orientation of nano-scaled structures in the specimen.

Second harmonic generation is a nonlinear optical process, in which two photons interacting with a polarizable material are effectively "combined" to form a new photon with twice the energy, and half the wavelength of the initial photons. It was first demonstrated by Franken et al. at the University of Michigan in 1961[2] and was only made possible by the invention of laser technology in 1960, which created the required high-intensity monochromatic light[3]. Every material which has a nonlinear dielectric coefficient and is transparent to both the fundamental optical frequency and the desired overtones is theoretical feasible for the production of optical harmonics[2]. Unlike fluorescence, these second harmonic signals are generated with no time delay at all and emerge temporally coinciding with the laser beam. The intensity of the resulting SH signal is of course dependent upon the particular material used, the role of the refractive indices in the harmonic process the frequency, polarization and intensity of the excitation light[4]. The SH signal is proportional to the square of the intensity of the excitation light[5]. In depth overviews of the theory lying behind the phenomenon of SHG can be found in the literature[6–8].

A number of highly organized nano-scaled biological structures have been reported that lack a center of optical symmetry and therefore behave as SHG-active non-linear photonic crystals[9,10]. The extracellular matrix protein collagen, posses a triclinic microcrystalline structure as shown by X-ray diffraction, has been shown to be the most efficient SHG source in tissues[11]. Another optical active resource is given by the sarcomers of skeletal muscle fibers, which are composed of myosin and actin with periods of 40 and 20 nm, respectively[12]. As both structures are highly represented in skeletal muscle, SHG microscopy should be a useful tool to study the resulting structural changes caused by the thermal treatment of muscle proteins and muscle-based foods.

In skeletal muscle, SHG arise from intrinsic proteins in the muscle fiber and the connective tissue. The coiled myosin rod domains have been identified as being the key structure for SHG. in skeletal muscle[13]. Collagens nonlinear dielectric coefficient were identified by Fukada and Yasuda[14] in bones, when they discovered that the dried tissue exhibited a significantly piezoelectric effect - a classic test of polarity in crystals. Later studies confirmed piezoelectric effects for the fibrillar collagens I, II and III in isolated fibrils and tissues, but not for nonfibrillar collagens like collagen IV[10]. Collagens produce SHG over a very broad optical excitation spectrum, covering several hundred nanometers[11]. No spectral dependence of the signals from the different collagen types could be identified so far. Nevertheless, the intensity of the signal exhibited by SHG has been thought to be much weaker for collagen type III compared to collagen type I and II[15]. In collagen molecules, three α chains are connected by hydrogen bonds between the NH of the glycine and the CO of the proline in the X

position of a neighboring α chain and thus create a helical ladder in the middle of the triple helix, which gives rise to the nonlinear dielectric coefficients. As a result of sum frequency vibrational spectroscopy, Mendoza et al. (2007) identified recently two molecular groups contributing to the signal by an approximately equal order of magnitude[16]. The outside orientated methylene groups, located in the pyrrolidine rings of proline and hydroxyproline amino acids residues, produce a nonlinear effect, as their alignment is characterized by a small, yet distinctive tilt relative to the main axis of the collagen fiber. The other contribution is given by carbonyl groups.

Helix coil transitions of muscle-based proteins induced by heating have been investigated with various techniques including differential scanning calorimetry, light scattering, and NMR[17–19] usually on soluble collagen or type I collagen from tendon. Similar methods have been used to study thermal denaturation behavior of myosin[20–22] and actin[23,24]. Nevertheless, most of these methods require extraction and solubilization of the protein of interest and are neither applicable for the investigation of complex tissues nor do they allow for simultaneous observation of ongoing structural changes at the required optical resolution. SHG laser scanning microscopy has several advantages when applied to imaging of tissue. As a result of the longer wavelength of the excitation, light imaging as deep as 900 μm into tissue is possible. Due to the non-linear nature of the excitation, the excitation volume is confined to a sub-micrometer slice (for a high numerical aperture objective) and thus SHG microscopy has an inherent optical sectioning capability. This allows for high-resolution imaging of thick meat specimen in 3D without the need for any additional labeling, which is an advantage as no further manipulation will interact with the system. The temporal resolution obtained by SHG imaging is given by the image acquisition time which for the present system is on the order of some tenths of seconds[25].

In the present paper we exploit the benefits of SHG microscopy to in situ investigation of structural changes of fibrous and myofibers as function of temperature and time in order to obtain temporally and spatially resolved data thus enabling a more complete understanding of the thermal denaturation process.

Materials and Methods

Materials

Fresh samples of M. biceps femoris of commercially slaughter pigs were dissected 24-h post-mortem and stored on ice in a refrigerator at 4°C until further processing. All chemicals were purchased at Sigma Aldrich (St. Luis, USA).

Sample Preparation

For microscopy small bundles of muscle tissue and small pieces of epimysium were dissected from the muscle using a dissection microscope. In order to allow for sufficient shrinkage but to still avoid free floating of the samples, the samples were loosely glued to a small window cut into aluminum foil pieces. They were then placed between two coverslips in a custom-made modified Olbrich chamber with a sufficient amount of 100-mM phosphate-buffered saline pH5.8.

Microscopy

The images were made using a custom-built multiphoton excitation microscope (Figure 1). The microscope is build around an Olympus IX70, which was specially optimized for laser scanning, two photon, and second harmonic imaging[25]. The microscope is coupled with a Spectra Physics (Mountain View, CA, USA) Mai-Tai (wideband Mai-Tai, 720–990 nm) Ti:sapphire femtosecond laser for the two-photon excitation experiments. The excitation wavelength was 780 nm and was circularly polarized. An Olympus ×40 water objective NA 0.9 was used. As the forward transmitted and the backscattered light reveal different features, care was taken to collect both the transmitted and the backscattered light. The transmitted light was collected by a ×20 Olympus air objective and passed through a multiphoton emitter (Chroma ET680SPUV) and a 3-mm thick BG12 filter and collected by the upper photomultiplier (PMT) in Figure 1. The back scattered light was passed through a multiphoton emitter (Chroma ET680sp) and a 400±10 nm band pass filter and collected by the lower PMT in Figure 1. The microscope was controlled by "Globals for imaging", software developed by Enrico Gratton at LFD at the University of California, Irvine.

Heating Experiments

The samples were heated on the microscope stage from 25°C to 70°C at an approximate rate of 1°C min^{-1}. The internal temperature of the chamber was recorded using a FLUKE 51 II thermometer coupled to a type K thermocouple. Images were recorded continuously at rate of 0.75 frames per second.

Image Processing and Analysis

Conversion of images into gray scale or false coloring was performed in Adobe Photoshop C 5 (Adobe Systems Incorporated, San Jose, CA, USA). Sarcomere length of myofibers were determined using Image Pro Plus software (Media Cybernetics, Silver Spring, MD, USA).

DSC

The thermal properties of the samples were measured using a sensitive Micro DSC III calorimeter, SETARAM (Caluire, France) with water as external cooling medium. Calibration of heat flow and temperature was performed with naphthalene (T_m=80.3°C, ΔH_{fus}=145.5 J g^{-1}). An aliquot of ~100 mg tissue samples was transferred to an inert metal vessel with 100 mM phosphate-buffered saline and hermetically closed. All samples were loaded onto the DSC instrument at 25°C and then cooled to 4°C before being

Fig. 1 Configuration of a custom-built microscope for simultaneous recording of forward and backscattered SHG. The transmitted light was collected by a ×20 Olympus air objective and passed through a multiphoton emitter (Chroma ET680SPUV) and a 3-mm thick BG12 filter and collected by the upper photomultiplier (PMT). The backscattered light was passed through a multiphoton emitter (Chroma ET680sp) and a 400±10 nm band pass filter and collected by the lower PMT. The microscope was controlled by "Globals for imaging", software developed by Enrico Gratton at LFD at the University of California, Irvine
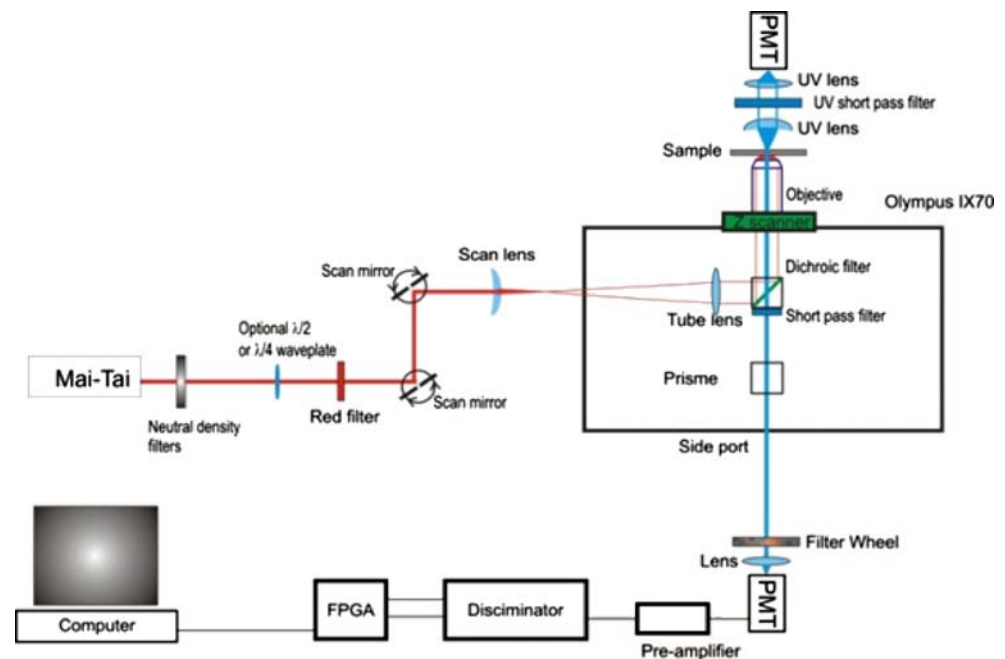
heated to 75 °C at a rate of 0.2 °C min^{-1}. A second cooling cycle to 4 °C and reheating to 75 °C was performed at the same rate as the first one in order to test for reversibility upon cooling. The experimental conditions were identical for all tissues.

Results

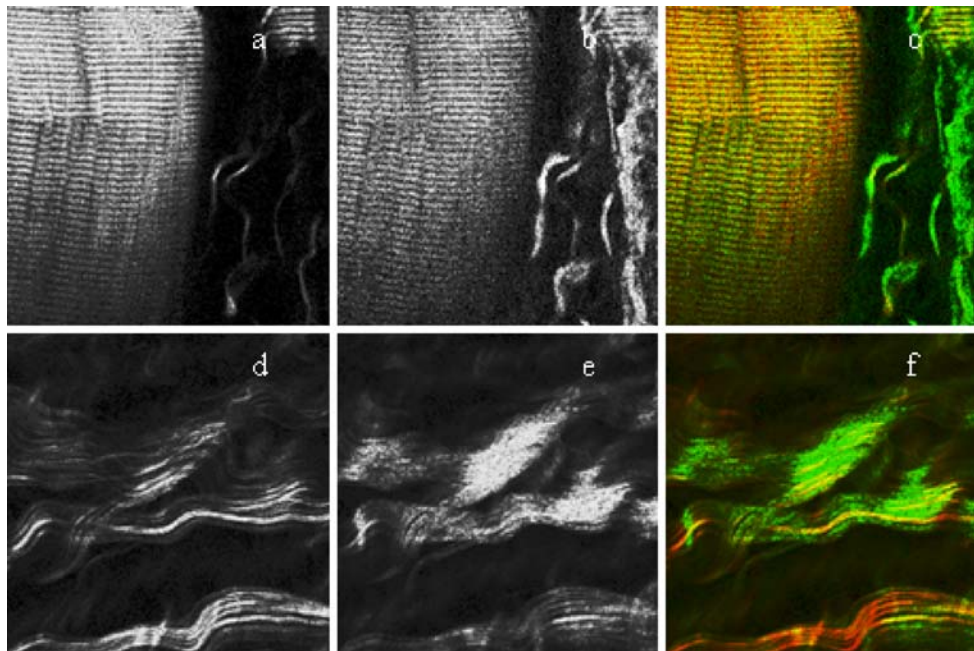### Forward Versus Backscattered SHG Microscopy

Forward and backscattered SHG microscopy results in the visualization of different features within the same sample. In the images of muscle fiber bundles (Figure 2a–c), the striated appearance of the myofibers due to their segmentation into sarcomers is readily observable in both the forward (Figure 2a) as well as the backscattered images (Figure 2b). Adjacent collagen fibers can also be perceived in both modes, but in the backscattered SHG micrographs more collagen fibers and of larger dimensions are present. Additionally, differences in the relative intensities between the two modes exist. In the forward mode, the relative intensity of the myofibers is higher than the one for the collagen fibers, while in the backscattered images the opposite is the case. With the RGB coding used in this presentation, co-localized signal intensities with almost the same weights would add up to

yellow color in the merged images (Figure 2c). The largest part of the collagen fibers emerges in green with only a few small yellow and some even smaller red areas, meaning that the intensity of the backward scattered light is dominating. Forward and backscattered signals contribute almost equally to the merged image of myofibers, but also here the signals are only partly co-localized as a pattern of yellow, red, and greed stripes can be seen.

SHG microscopy of epimysium (Figure 2d–f) shows parallel structures of wavy collagen fibers. While the image of the forward SHG (Figure 2d) appears as better resolved, the images of the backscattered collagen displays larger areas of higher intensities (Figure 2e.). In the merged image (Figure 2f) only a few fibers are equally presented in both modes and the majority of the collagen structures displayed originate from the backscattered image.

SHG Microscopy Reveals that Thermal Denaturation of Constituents in the Muscle Fibers Takes Place at Lower Temperatures than Denaturation of Collagen Fibers

The effect of thermal denaturation on major muscle structures was investigated by heating of small muscle fiber bundles on the microscope stage while imaging. Due to the observed differences in the resulting images between the two optical set ups, all following results are shown as

Fig. 2 Forward and backscattered SHG microscopy results in the visualization of different features within the same sample. The images show SHG from a muscle fiber bundle (a–c) as well as from epimysium (d–f) and are generated from forward propagated SHG (a, d) and backscattered SHG (b, e). In each case, the two recordings are merged in one image by using false coloring of forward SHG in red and backscattered SHG in green. Areas of perfect co-localization between the two signals appear in yellow (c and f). The images obtained by forward SHG are better resolved and show a higher intensity compared to the backscattered images. In the backscattered image of the muscle fiber bundle (b) more collagen fibers can be perceived than in the forward mode. Image sizes correspond to 110× 110 μm (a–c) and 146×146 μm (d–f)
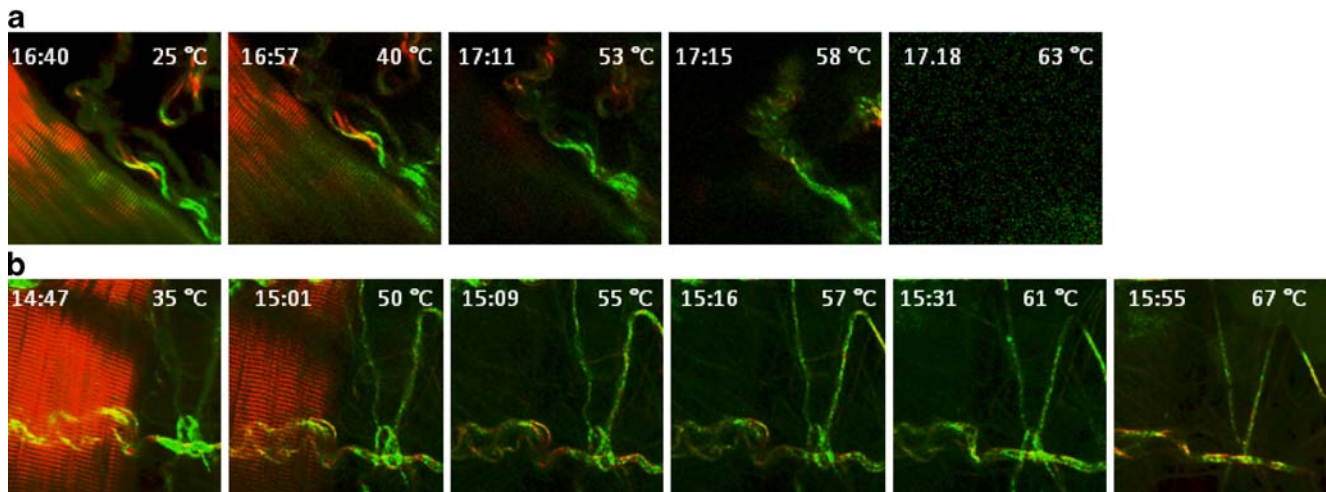
Fig. 3 Heat denaturation in muscle fibers takes place at lower temperatures than in collagen. Sequence of images recorded during heating of small myofiber bundles. The time and temperature profile are given on the images, and all images shown are merged images from forward (*red*) and backscattered (*green*) SHG. **a** The thermal behavior of a muscle fiber and adjacent collagen fibers can be observed. No structural changes can be detected until 53 °C, where the signal from the myofibers vanishes. Shrinkage and coiling of collagen fibers can be seen at 58 °C. At 63 °C the denaturation of the signal providing structures is complete. **b** Muscle fiber with vasculature and adjacent collagen fibers. No changes can be observed until 55 °C, were the signal from the myofiber has disappeared. Beginning shrinkage of collagen fibers occurs at 57 °C. However, here the SHG of the collagen in the vascular structures remains even after heating to 67 °C for a prolonged time. Images shown have a size of 110×110 μm

merged images (Figures 3 and 5). In muscle fiber bundles, a decrease in the intensity of the SHG signal can already be seen at 40 °C, before the muscle fibers vanish at 53 °C (Figure 3a and b). No prior structural changes can be observed. At 57 °C, severe shrinkages take place in restrained collagen fibers while non-attached collagen fibers begin to coil up (Figure 3b). The SHG signal from most collagen fibers becomes extinct between 59 °C and 60 °C (Figure 4). However, we also found muscle fiber bundles in which certain collagen fibers continued to exhibit signal even after prolonged heating at elevated temperature (Figure 3b).

As a control for the thermal behavior of collagen fibers also thin samples of epimysium (Figure 5) were heated. Here as well, severe shrinkage becomes visible at 57 °C and the signal vanishes at 59 °C (Figure 5a). Imaging of the same structure after cooling of the sample on the microscope showed that no reformation of SHG producing structures occurs. Yet, as in the case of the muscle fiber bundle, also here some areas with collagen fibers still exhibiting SHG signals after heating (Figure 5b) were found. In collagen structures as well, a general loss of signal intensity can be observed around 40 °C.

DSC Thermograms Show Endothermic Reaction at Temperatures Corresponding to SHG Microscopy

Figure 4 shows the micro DSC thermograms of a suspension of small myofiber bundles. The material shows a series of overlapping endothermic transitions in the temperature interval of interest (45–65 °C). This set of transitions, which are not reversible as they are not seen in the second upscan, are traditionally within food science attributed to myosin. The first partly resolved endotherm coincides with the disappearance of SHG signal from myofibers. In the interval between 55 °C and 60 °C, a second endothermic transition is observed coinciding with first shrinkage of collagen fibers (57 °C) and then melting of collagen fibers (59 °C) as seen by disappearance of SHG signal (Figure 3a).
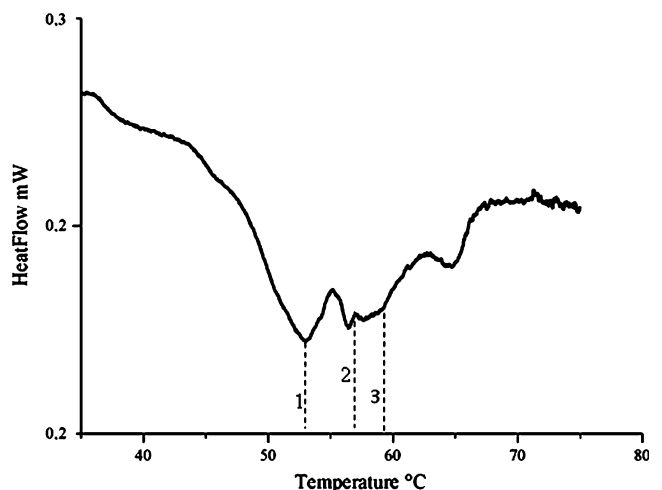

Fig. 4 Thermogram of a small myofiber bundle. The vertically orientated *dashed lines 1–3* refer to temperatures were major structural changes could be observed by SHG microscopy. *Line 1* corresponds to the disappearance of the SHG signal from myofibers, *line 2* matches the onset of shrinkage in collagen fibers while *line 3* indicates the melting point of collagen fibers in muscle tissue
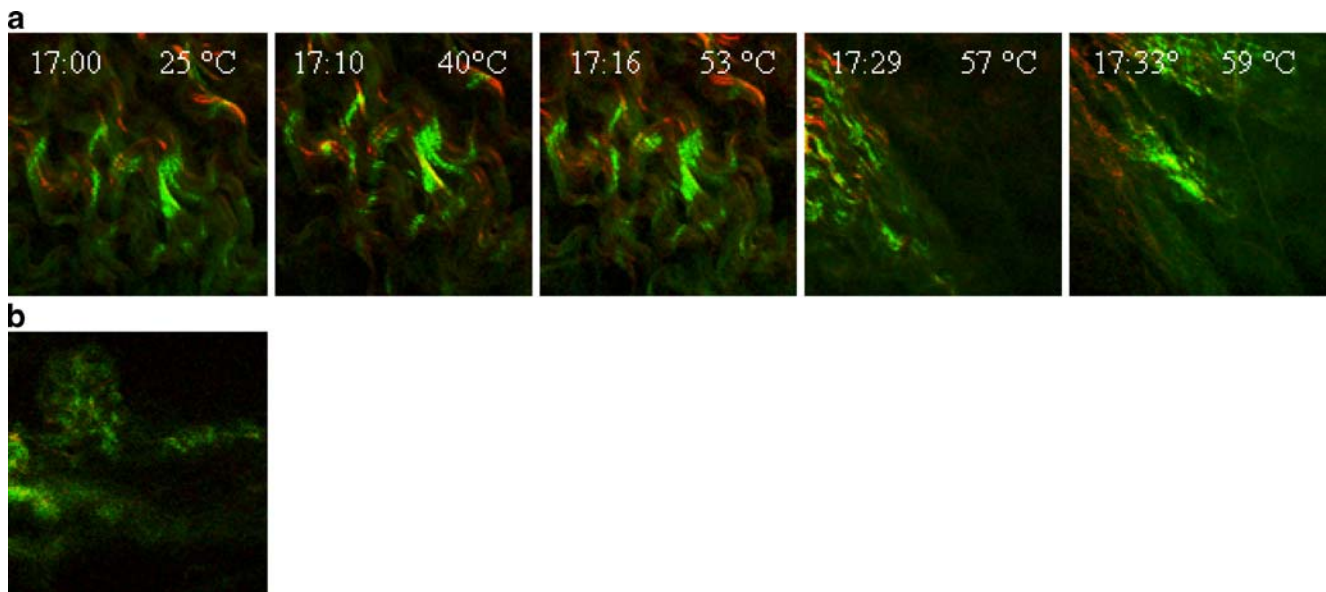
Fig. 5 Temperature profile of structural changes in epimysium corresponds to the one observed in muscle fiber bundles. All images shown are merged images from forward (*red*) and backscattered (*green*) SHG. **a** Sequence of images taken during heating of epimysium. Time and temperature are indicated on the respective image. No changes can be observed until 57°C, where severe shrinkage of all collagen fibers occurs. The SHG signal begins to vanish at 59°C. No signal. **b** Remaining SHG of vascular structures in a different field of view in epimysium after heating to 65°C. Image sizes 146×146 μm

In Figure 6a thermogram of epimysium is shown. In contrast to the more complex picture of myofibers epimysium shows only a single endothermic transition. The onset of this transition coincides with shrinkage of collagen fiber and peak temperature coincides with melting of collagen structure observed as complete loss of SHG signal (Figure 5a).
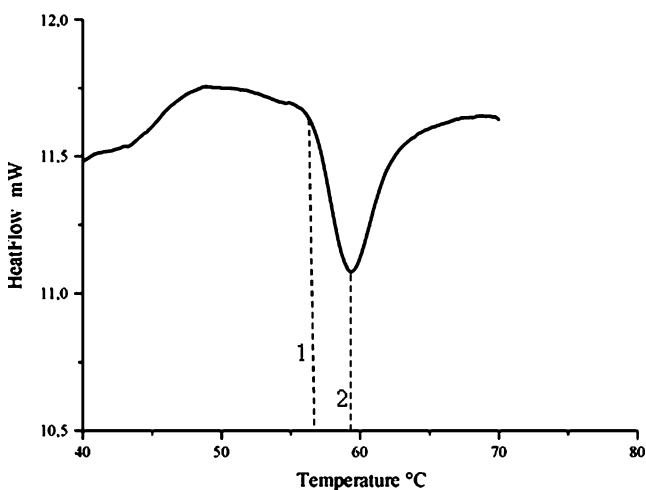
Fig. 6 Thermogram of epimysium. *Line 1* corresponds to the temperature were shrinkage in collagen fibers in epimysium was observed, while *line 2* indicates the melting temperature for the majority of the collagenous structures as taken from SHG microscopy

Discussion

The observed difference between forward and backward collected SHG images of the present study can be rationalized in terms of the fundamental principles of second harmonic generation, the implementation of the experimental setup and the sample being imaged[4,26]. For a collagen fiber bundle lying nearly normal to the incident excitation light, (as is the case in Figures 2 and 5) the dipole moment of the collagen is also near normal to the incident light and can radiate both forward and backward. However, due to conservation of the momentum of the excitation photons most of the second harmonic will propagate in the forward direction (i.e. the direction of the excitation laser). Some smaller amount of SHG will be made by scattered excitation photons, the resulting SHG from this process will be weaker and more diffuse then the forward moving SHG. Yet, because of the different optical path ways the photons have to travel, any SHG from scattered excitation light traveling forward will be negligible due to scattering in the sample and the lower NA objective used in this experiment to collect the forward moving SHG. This will result in only the non-scattered SHG reaching the detector and thus a better resolved image. In the case of the backward moving SHG the high NA is very efficient at collecting the scattered light resulting in a more diffuse image.

The different behavior of the SH signal from the collagen and the myofibers is due to the fundamental difference in structure between the collagen and the

myofibers. The myofibers are well ordered over long distances allowing for constructive interference of the forward propagating SH signal. This in turn results in a more intense forward propagating SH signal as is seen in Figure 2a and b. Collagen, on the other hand, is only well ordered over short distances, this leads to less constructive interference for the SH signal and more scattered SH light. Therefore the forward propagating SH signal from collagen is found to be less intense than that of the backscattered SH signal (Figure 2d–e).

Thermal-Induced Changes in Muscle Proteins

For proteins in solution the denaturation can be followed by several techniques which monitor changes in size, shape, or configuration of the macromolecules. In case of insoluble fibers and complex tissues, relatively few techniques are available to follow the process at the required resolution. In the past, DSC was most commonly used in order to study thermal-induced denaturation of muscle tissue. The results indicated that thermal transitions in muscle can be localized in mainly three temperature ranges, which are above 45°C: T_1 (45–60°C, T_{max}=54°C) is attributed to myosin; T_2 (60–76°C, T_{max}=65°C) is attributed to sarcoplasmatic proteins, actomyosin, and connective tissue proteins; and T_3 (76–92°C, T_{max}=80–85°C)[27,28]. DSC analysis of intramuscular connective tissue resulted in one transition between 40°C and 63°C[29]. All investigations showed a strong interdependence between the transition temperature, the ionic environment and heating rate applied. In complex tissues, such methodologies based on the macroscopic heat flow in and out of the whole sample will often produce results that leave room for multiple interpretations terms of assigning the individual proteins to observed endotherms and this remains subject of vigorous debate.

Using SHG microscopy of muscle fibers, it has been demonstrated that thermal denaturation of the myosin rod domain is starting already at temperatures below 40°C as the signal intensity is clearly reduced and that denaturation is complete at 53°C. Though SHG microscopy is an inherent quantitative process, the experimental set up used in this experiment does not allow for precise quantification of the signal intensities. Heating of the samples can induce small motions, which could consequently lead to small shifts in the focal volume. However, other authors working on thin sections of heat-denatured collagen, observed a loss in SHG signal intensities of 25% from 25°C to the next step investigated at 50°C and a further loss up to 85% at 60°C[30]. Here as well, a similar trend in the development of the signal intensities could be observed between 25°C and 40°C.

A broad range of denaturation temperatures have been reported for collagen type I and the experimental set up has to be considered for the interpretation of the result achieved. In solution denaturation temperature ranges have been found to vary from 37°C to 72°C, primarily depending on the heating rate applied[31,32]. Using microscopy, most authors observed denaturation temperatures in the range between 57°C and 65°C in tendons and skin[33–35]. In all cases, hydrothermal shrinkage of collagen fibers up to 70% of the original length, demarking the onset of the helix coil transition, has been recognized as a characteristic of the molecule. Flory and Garret described collagen denaturation as a melting process, a proposal that earned such wide acceptance that the word melting is commonly used synonym with denaturation or unfolding to denote the helix coil transition of collagen[36]. They considered melting as an equilibrium process, while Miles et al. proposed a kinetic view in which the denaturation is governed by an irreversible process transforming native collagen into a denatured state with a highly temperature-dependent rate[17].

The kinetic view leads consequently to a model of domains with variable thermal stabilities along the length of the molecule and can explain the observed DSC scan rate dependencies. Partially uncoupling of the individual alpha chains in the hydroxyproline-deficient sequences is thought to be the starting point of the transition, before the whole structure unfolds. The hydroxyproline-free region in a single collagen I molecule is comprising of approximately 65 residues. However, in the quarter-staggered end-overlap arrangement of fibrils, this size is reduced to 26 residue in the gap regions due to interaction with neighboring molecules[37]. Collagen molecules embedded within the lattice of a fiber are substantially more thermally stable than the same molecules in dilute solutions. The data and images presented here support the model of Miles et al. as the denaturation is seen to be an irreversible process and the rate of denaturation is also found to be temperature dependent.

In conclusion, it has been shown that SHG microscopy can be used as a noninvasive imaging method for muscle and collagen tissue and that SHG microscopy has the potential to provide unique additional information in the analysis of muscle-based foods. It is shown that the SHG signal is highly sensitive to the denaturation of both myo- and collagen fibers. In fact the SHG signal could register changes in intensity at temperatures as low as 40°C corresponding to slow irreversible denaturation while the DSC analysis only provides less informative information in terms of a series of overlapping endothermic transitions starting at temperatures above 45°C. SHG microscopy of heat-treated muscle and connective tissue confirmed principally the irreversibility of the helix coil transition upon cooling, but revealed also that large local variability of the thermal stability of collagenous structures in skeletal muscle. Such variability will not be detected by techniques which rely on spatial averaging over the entire sample. In skeletal muscle connective tissue, fibrous collagen can be

found in a variety of different elements like different vascular or nervous structures. Further systematic studies using SHG microscopy are necessary in order to identify the structural origin of the variations of the collagen thermal behavior.

References

1. D.A. Bruggemann, M.A. Lawson, J. Fish Biol. **66**, 810 (2005)
2. P.A. Franken, G. Weinreich, C.W. Peters, A.E. Hill, Phys. Rev. Lett. **7**, 118–119 (1961)
3. T.H. Maiman, Nature **187**, 493 (1960)
4. R.M. Williams, W.R. Zipfel, W.W. Webb, Biophys. J. **88**, 1377 (2005)
5. P.A. Franken, J.F. Ward, Rev. Mod. Phys. **35**, 23 (1963)
6. N. Bloembergen, *Nonlinear Optics* (World Scientific, Hackensack, 1996)
7. Y.R. Shen, *The Principles of Nonlinear Optics* (Wiley, New York, 2003)
8. F. Zernike, J.E. Midwinter, *Applied Nonlinear Optics* (Dover, Mineola, 1973)
9. S. Fine, W.P. Hansen, Appl. Opt. **10**, 2350 (1971)
10. W.R. Zipfel, R.M. Williams, R. Christie, A.Y. Nikitin, B.T. Hyman, W.W. Webb, Proc. Natl Acad. Sci. USA **100**, 7075 (2003)
11. E. Georgiou, T. Theodossiou, V. Hovhannisyan, K. Politopoulos, G.S. Rapti, D. Yova, Opt. Commun. **176**, 253 (2000)
12. P.-C. Cheng, C.K. Sun, in *Handbook of Biological Confocal Microscopy*, 3rd edn., ed. by J.B. Pawley (Springer, Singapore, 2006), p. 703
13. S.V. Plotnikov, A.C. Millard, P.J. Campagnola, W.A. Mohler, Biophys. J. **90**, 693 (2006)
14. E. Fukada, I. Yasuda, J. Phys. Soc. Jpn. **12**, 1158 (1957)
15. G. Cox, E. Kable, A. Jones, I.K. Fraser, F. Manconi, M.D. Gorrell, J. Struct. Biol. **141**, 53 (2003)
16. I. Rocha-Mendoza, D.R. Yankelevich, M. Wang, K.M. Reiser, C.W. Frank, A. Knoesen, Biophys. J. **93**, 4433 (2007)
17. C.A. Miles, T.V. Burjanadze, A.J. Bailey, J. Mol. Biol. **245**, 437 (1995)
18. A. Rochdi, L. Foucat, J.P. Renou, Biopolymers **50**, 690 (1999)
19. E.I. Tiktopulo, A.V. Kajava, Biochemistry **37**, 8147 (1998)
20. H.C. Bertram, Z.Y. Wu, F. van den Berg, H.J. Andersen, Meat Sci. **74**, 684 (2006)
21. H.H. Wang, M. Pato, Z. Pietrasik, P. Shand, Food Chem. **113**, 21 (2009)
22. T. Brenner, R. Johannsson, T. Nicolai, Food Hydrocoll. **23**, 296 (2009)
23. D.I. Levitsky, A.V. Pivovarova, V.V. Mikhailova, O.P. Nikolaeva, Febs Journal **275**, 4280 (2008)
24. C.R. Gicquaud, B. Heppell, Biopolymers **83**, 374 (2006)
25. J. Brewer, M. Schiek, A. Lutzen, K. Al-Shamery, H.G. Rubahn, Nano Lett. **6**, 2656 (2006)
26. J.X. Cheng, A. Volkmer, X.S. Xie, J. Opt. Soc. Am., B, Opt. Phys. **19**, 1363 (2002)
27. D.J. Wright, I.B. Leach, P. Wilding, J. Sci. Food Agric. **28**, 557 (1977)
28. E. Stabursvik, H. Martens, J. Sci. Food Agric. **31**, 1034 (1980)
29. N. Aktas, Thermochim. Acta. **407**, 105 (2003)
30. T.A. Theodossiou, C. Thrasivoulou, C. Ekwobi, D.L. Becker, Biophys. J. **91**, 4665 (2006)
31. E. Leikina, M.V. Mertts, N. Kuznetsova, S. Leikin, Proc. Natl Acad. Sci. USA **99**, 1314 (2002)
32. A. Finch, D.A. Ledward, Biochim. Biophys. Acta. **278**, 433 (1972)
33. T. Theodossiou, G.S. Rapti, V. Hovhannisyan, E. Georgiou, K. Politopoulos, D. Yova, Lasers Med. Sci. **17**, 34 (2002)
34. I. Zsnagy, V.N. Toth, F. Verzar, Connect. Tissue Res. **2**, 265 (1974)
35. A. Ewald, Hoppe-Seylers Zeitschrift fur Physiologische Chemie **105**, 115 (1919)
36. P.J. Flory, R.R. Garrett, J. Am. Chem. Soc. **80**, 4836 (1958)
37. C.A. Miles, A.J. Bailey, Micron **32**, 325 (2001)